UDK 621.941:004.032.26
Original scientific article/Izvirni znanstveni članek

ISSN 1580-2949
MTAEC9, 48(2)227(2014)

EXPERIMENTAL DESIGN AND ARTIFICIAL NEURAL NETWORK MODEL FOR TURNING THE 50CrV4 (SAE 6150) ALLOY USING COATED CARBIDE/CERMET CUTTING TOOLS

EKSPERIMENTALNA ZASNOVA IN MODEL UMETNE NEVRONSKE MREŽE ZA STRUŽENJE JEKLA 50CrV4 (SAE 6150) Z UPORABO ORODIJ S KARBIDNO ALI KERMETNO PREVLEKO

Murat Tolga Ozkan[1], Hasan Basri Ulas[2], Musa Bilgin[3]

[1]Gazi University, Faculty of Technology, Department of Industrial Design Engineering, 06500 Ankara, Turkey
[2]Gazi University, Faculty of Technical Education, Mechanical Education Department, 06500 Ankara, Turkey
[3]Erzincan University, Vocational Technical School, Mechanical Program, 24000 Erzincan, Turkey
mtozkan06@yahoo.com

Prejem rokopisa – received: 2013-03-08; sprejem za objavo – accepted for publication: 2013-06-18

In this experimental study, the 50CrV4 (SAE 6150) steel was subjected to the machining tests with coated carbide and cermet cutting tools in a turning operation. The tests were carried out at various cutting speeds, feed rates and cutting depths. In the light of these parameters, cutting forces and surface-roughness values were determined. Three components (F_a, F_r and F_c) of the cutting forces were measured during the tests using a dynamometer, while the machined surface-roughness values were determined using a surface roughness measuring unit. A multiple regression analysis and experimental design were performed statistically. The measured surface-roughness values were used for the modeling with an artificial neural network system (ANNS). The relations between the cutting forces and the surface-roughness values were also defined.

Keywords: turning operations, coated carbide/cermet cutting tools, cutting force, surface roughness, artificial neural network

V tej študiji je bilo jeklo 50CrV4 (SAE 6150) strojno obdelano s struženjem z orodji za rezanje s karbidno ali kermetno prevleko. Preizkusi so bili opravljeni pri različnih hitrostih rezanja, podajanja in globine rezanja. Iz teh parametrov so bile ugotovljene sile pri rezanju in vrednosti hrapavosti površine. Tri komponente sil rezanja (F_a, F_r in F_c) so bile merjene med poskusom z dinamometrom, medtem ko so bile vrednosti hrapavosti površine izmerjene z merilnikom za hrapavost površine. Izvršena je bila večkratna regresijska analiza in statistična obdelava izvedbe poskusov. Izmerjene vrednosti hrapavosti so bile uporabljene za modeliranje s sistemom umetne nevronske mreže (ANNS). Določena je bila tudi odvisnost med silami rezanja in hrapavostjo površine.

Ključne besede: postopek struženja, rezilna orodja s karbidno ali kermetno prevleko, sila rezanja, hrapavost površine, umetna nevronska mreža

1 INTRODUCTION

Machining experiments are usually costly and time consuming. In order to eliminate the cost and to reduce the time, some advanced techniques were developed. These are generally called modeling. There are several modeling methods. Empirical modeling, analytical modeling, mechanistic modeling, finite-element modeling and artificial neural network modeling are some of these modeling methods. With these techniques, predictions are made using the experimentally obtained results.

Boubekri et al.[1] investigated different cutting conditions on three grades of steel, namely, 1018 (low-carbon, cold-rolled steel), 304 (austenitic stainless steel) and 4140 (low-alloy steel) using uncoated carbide inserts as the tool material. Mathematical models were developed for predicting the forces acting on the tool for different cutting conditions and materials.

Kumar et al.[2] studied the performance of an alumina-based ceramic cutting tool as an attractive alternative for carbide tools in the machining of steels in its hardened condition. Two types of ceramic cutting tools, namely, the Ti[C, N] mixed alumina-ceramic cutting tool and zirconia-toughened alumina-ceramic cutting tool were used for the investigation. The performance of these ceramic cutting tools related to the surface finish was also discussed.

Tekiner and Yeşilyurt[3] carried out machining tests to determine the best cutting conditions and cutting parameters in the turning of AISI 304 stainless steels by taking into consideration the process sound. The ideal cutting parameters and cutting-process sounds were determined.

The tests involving the AISI 4340 steel were performed using two hardness values, 42 HRC and 48 HRC; for the former, a coated carbide insert was used as the cutting tool, whereas for the latter a polycrystalline cubic boron nitride insert was employed. The machining tests on the AISI D2 steel hardened to 58 HRC were conducted using a mixed-alumina cutting tool. The cutting forces, surface roughness, tool life and wear mechanisms were assessed. The results indicated that when turning

the AISI 4340 steel, using low feed rates and depths of cut, the forces were higher when machining the softer steel and that the surface roughness of the machined part was improved as the cutting speed was elevated and it deteriorated with the increasing feed rate.[4]

The wear mechanisms of the cutting tools made of tungsten-carbide (WC), PCBN and PCD were investigated using the tool life and the temperature results available in the literature. For the tool/work combinations of WC/steel and PCBN/hardened-steel, under practical conditions, the tool wear was found to be greatly influenced by the temperature.[5]

The AISI 4340 low-alloy steel was assumed for the workpiece. Cubic boron-nitride (CBN) or polycrystalline (PCBN) inserts are widely used as the cutting-tool material in high-speed machining of hardened tool steels due to high hardness, high abrasive-wear resistance and chemical stability at high temperature. Cutting forces and feed forces were determined with numerical simulations. The cutting force and feed force increased with the increasing feed, tool-edge radius, negative rake angle, and workpiece hardness. The results from the simulations were compared to the experimental results reported in the literature.[6]

The effects of the cutting speed, cutting force and feed rate on the flank wear land and tool life of the TiN coated carbide inserts in boring operations were studied when machining the 38MnVS5 alloy. The results showed that the machinability of microalloyed steel is better than that of heat-treated alloy steels under identical conditions.[7]

The tribological influences of PVD-applied TiAlN coatings on the wear of cemented carbide inserts and the microstructure influence on the wear behaviors of the coated tools were investigated under dry and wet machining. The turning test was conducted with variable high cutting speeds ranging from 210 m/min to 410 m/min.[8]

The tested work materials were plain carbon steel JIS S45C and BN free-machining steels. The JIS S45C was used as the standard. The tool wear in turning the BN free-machining steel was smaller than that in turning the standard steel. In the case of turning BN1 with P30 at 200 m/min, 300 m/min, the wear-progress rate of the flank wear and crater depth were about half as much as that in turning the standard steel. The BN free-machining steel showed a slightly lower cutting temperature and a smaller cutting force in comparison with the standard steel at the tested cutting speeds.[9]

The cutting-force data used in the analyses was gathered with a tool-breakage detection system detecting the variations of the cutting forces measured with a three-dimensional force dynamometer. The workpiece materials used in the experiments were: cold-work tool steel, AISI O2 (90 MnCrV8); hot-work tool steel, AISI H10 (X32CrMo33); and mould steel, AISI improved 420 (X42Cr13). The cutting tools used were HSS tools, uncoated WC and coated TiAlN and TiC + TiCN + TiN inserts (ISO P25). No cutting fluid was used during the turning operations. During the experiments, the cutting forces, flank wear and surface-roughness values were measured throughout the tool life and the machining performances of the tool steels were compared.[10]

Orthogonal cutting experiments were performed on a high-speed machining center with the surface speeds of up to 500 m/min and the uncut chip thicknesses ranging from 0.1 mm to 0.3 mm. The results indicate that in certain critical regions of the thermal field, the improved machinability correlates with significant reductions in the temperature exceeding the measurement uncertainties. Such micro-scale temperature measurements will help to design the materials with further improved machinability.[11]

Three different carbide cutting tools were used, namely, TiCN + TiC + TiCN + Al_2O_3 + TiN-coated carbide tools with multilayer coatings of 7.5 μm and 10.5 μm and an uncoated WC/Co tool. The turning experiments were carried out at four different cutting speeds, which were (125, 150, 175 and 200) m/min. The feed rate (f) and depth of cut (a_p) were kept fixed at 0.25 mm/r and 1.5 mm/r, respectively, throughout the experiments. The tool performance was evaluated with respect to the tool wear, the surface finish produced and the cutting forces generated during turning.[12]

Cakir and Isik[13] performed a study about the tool-life testing with single-point turning tools. The cutting-force data used in the analysis was gathered with a tool-breakage detection system detecting the variations of the cutting forces measured with a three-dimensional force dynamometer. Six pairs of ductile iron specimens, austempered at (300, 350 and 400) °C for 1 h and 2 h were tested. The cutting tools used in the tests were coated carbide inserts, ISO SNMG 120408 (K10), clamped on the tool holders, CSBNR 2525 M12. No cutting fluid was used during the turning operations. During the experiments, the cutting forces, flank wear and surface-roughness values were measured throughout the tool life and the machining performances of ADI having different structures were compared.

Lalwani et al.[14] carried out a machining study focusing on the effect of the cutting parameters (cutting speed, feed rate and depth of cut) on the cutting forces (feed force, thrust force and cutting force) and the surface roughness in the finish hard turning of the MDN250 steel (equivalent to the 18Ni(250) maraging steel) using a coated ceramic tool. A non-linear quadratic model best describes the variation in the surface roughness with the major contribution of the feed rate and the secondary contributions of the interaction effect between the feed rate and the depth of cut, the second-order (quadratic) effect of the feed rate and the interaction effect between the speed and depth of cut. The suggested models of the cutting forces and surface roughness are adequately map-

ped within the limits of the cutting parameters considered.

In another study, coated tungsten-carbide ISO P-30 turning-tool inserts were subjected to a deep cryogenic treatment (–176 °C). The machining studies were conducted on a C45 workpiece using both untreated and deep cryogenic treated tungsten-carbide cutting-tool inserts. The cutting force during the machining of the C45 steel is lower in the case of the deep cryogenic treated carbide tools when compared with the untreated carbide tools. The surface finish produced when machining the C45 steel workpiece is better with the deep cryogenic treated carbide tools than with the untreated carbide tools.[15]

The objective of the work is to determine the influence of cutting fluids on the tool wear and surface roughness during turning AISI 304 with a carbide tool. A further attempt was made to identify the influence of coconut oil on reducing the tool wear and surface roughness during the turning process. The performance of coconut oil was also compared with two other cutting fluids, namely, an emulsion and a neat cutting oil (immiscible with water).[16]

Ebrahimi and M. M. Moshksar[17] machined microalloyed steel (30MnVS6) and quenched-tempered (QT) steels (AISI 1045 and AISI 5140) under different cutting conditions. An experimental investigation was conducted to determine the effects of the cutting speed, feed rate, hardness, and workpiece material on the flank wear and tool life of the coated cemented carbide inserts in the hard-turning process. A statistical analysis was used for evaluating different factors of the cutting forces. Chip characteristics and the chip/tool contact length were also investigated.

In another study, the machining of the uncoated AISI 1030 steel (i.e., the orthogonal cutting), PVD- and CVD-coated cemented carbide inserts with different feed rates of (0.25, 0.30, 0.35, 0.40 and 0.45) mm/r, with the cutting speeds of (100, 200 and 300) m/min and a constant depth of cut (i.e., 2 mm), without using a cooling liquid was accomplished. The effects of the surface roughness, the coating method, the coating material, the cutting speed and the feed rate on the workpiece were investigated. Afterwards, these experimental studies were carried out on artificial neural networks (ANNs). The training and test data of the ANNs were prepared using experimental patterns for the surface roughness. Therefore, the surface-roughness value was determined with an ANN with an acceptable accuracy.[18]

Gaitonde et al.[19] made a study analyzing the effects of the depth of cut and the machining time on the machinability aspects such as machining force, power, specific cutting force, surface roughness and tool wear using second-order mathematical models during turning high-chromium AISI D2 cold-work tool steel with the CC650, CC650WG and GC6050WH ceramic inserts.

The effects of the machining parameters on the cutting force, specific cutting pressure, cutting temperature, tool wear and surface-finish criteria were investigated during the experimentation. The present approach and the results will help manufacturing engineers to understand the machinability of Inconel 718 during high-speed turning.[20]

Two AISI 4140 steels with different machinability ratings and three types of tools were compared. The control-volume approach was used to estimate the energy partition from the thermal images and the energy outflows were compared for the measurement of the cutting power. This provides a new physical tool for examining machinability, tool wear and subsurface damage.[21]

The work is an experimental study of hard turning the AISI 52100 bearing steel with a CBN tool. The relationships between the cutting parameters (cutting speed, feed rate and depth of cut) and machining output variables (surface roughness, cutting forces) are analyzed and modeled with the response-surface methodology (RSM). Finally, the depth of cut exhibits the maximum influence on the cutting forces as compared to the feed rate and cutting speed.[22]

There are many studies in the literature about the artificial neural network modeling of the surface roughness. The main purpose of this study is to carry out the turning tests on the 50CrV4 (SAE 6150) steel using coated carbide/cermet cutting tools and to carry out the modeling with an artificial neural network. There are many studies in the literature about the SAE 6150 material. These studies are especially related to physical and mechanical properties. However, there is no sufficient study on the machinability of the SAE 6150 material.

2 MATERIALS AND METHOD

The turning tests were carried out on the commercially available 50CrV4 (equivalent to SAE 6150) steel workpiece specimens. These steel specimens were produces by CEMTAS, TR and their chemical composition is shown in **Table 1**.

The 50CrV4 (SAE 6150) workpiece specimens were prepared in accordance with the requirements of the ISO

Table 1: Workpiece material 50CrV4 (SAE 6150) and its chemical composition (*w*/%)
Tabela 1: Material obdelovancev 50CrV4 (SAE 6150) in njegova kemijska sestava (*w*/%)

Material	Hardness (HB)	Material content						
		C	Si	Mn	P	S	Cr	V
50CrV4 - SAE(AISI)6150	311	0.50	0.31	0.78	0.009	0.008	1.06	0.15

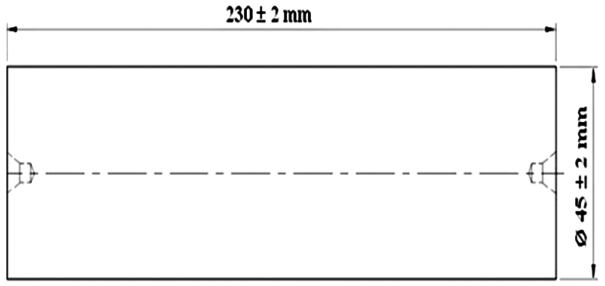

Figure 1: Experimental-workpiece-specimen geometry
Slika 1: Geometrija poskusnega vzorca

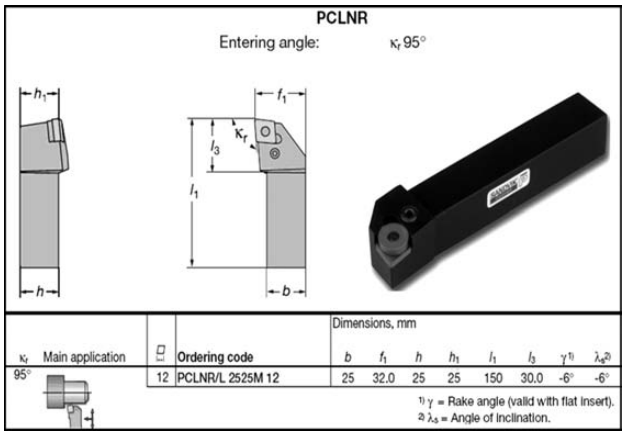

Figure 2: Tool-holder specifications
Slika 2: Specifikacija nosilca orodja

3685 standard. The size of the specimens was determined in accordance with the diameter/length ratio that should not exceed 1/10. Prior to the machining tests through a surface turning operation, both faces of the specimens were machined and center drilled on a universal lather. The dimensions of the workpiece specimens are shown in **Figure 1**.

Tool holder was also chosen according to the requirements specified in ISO 3685 for the machinability tests. The specifications of the tool holder, produced by SANDVIK, were PCLNR 2525 12. The tool-holder features are shown in **Figure 2**.

The cutting inserts with six different features were used for the machining tests. These cutting inserts were coated carbide and cermet cutting tools. In addition, the cutting-insert tip radii were (0.4, 0.8 and 1.2) mm. The cutting-insert grades and technical specifications are shown in **Table 2**.

The machining tests were carried out at the cutting speeds of (150, 200, 250, 250 and 300) m/min, the feed rates of (0.12, 0.16, 0.20) mm/r and the depths of cut of (0.5, 1, 1.5) mm without a coolant, using the cutting tools whose specifications are given in **Table 2**. The cutting speed, depth of cut and feed rate were chosen according to the manufacturer's recommendations, the

Table 2: Cutting-tool technical specifications
Tabela 2: Tehnične značilnosti poskusnega orodja za rezanje

Cutting-tool number	Cutting-tool material	Cutting tool	Coating method	Coating material	Code	Tip radius	ISO grade
1	Carbide		CVD	Al_2O_3+TiCN	GC4215	0.4	CNMG 12 04 04-PF-P15
2	Carbide		CVD	Al_2O_3+TiCN	GC4215	0.8	CNMG 12 08 04-PF-P15
3	Carbide		CVD	Al_2O_3+TiCN	GC4215	0.12	CNMG 12 12 04-PF-P15
4	Cermet		PVD	TiN+TiCN	GC1525	0.4	CNMG 12 04 04-PF-P15
5	Cermet		PVD	TiN+TiCN	GC1525	0.8	CNMG 12 08 04-PF-P15
6	Cermet	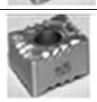	PVD	TiN+TiCN	GC1525	0.12	CNMG 12 12 04-PF-P15

Table 3: Cutting parameters used in the experimental study
Tabela 3: Parametri rezanja, uporabljeni pri eksperimentih

Cutting tool	Tip radius R_ε/mm	Depth of cut d/mm	Feed rate f/(mm/r)	Cutting speed v/(mm/min)
Coated carbide	0.4–0.8–1.2	0.5–1–1.5	0.12–0.16–0.20	150–200–250–250–300
Coated cermet	0.4–0.8–1.2	0.5–1–1.5	0.12–0.16–0.20	150–200–250–250–300

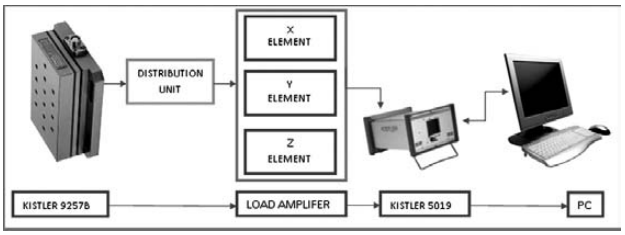

Figure 3: Schematic presentation of the experimental assembly
Slika 3: Shematski prikaz eksperimentalnega sestava

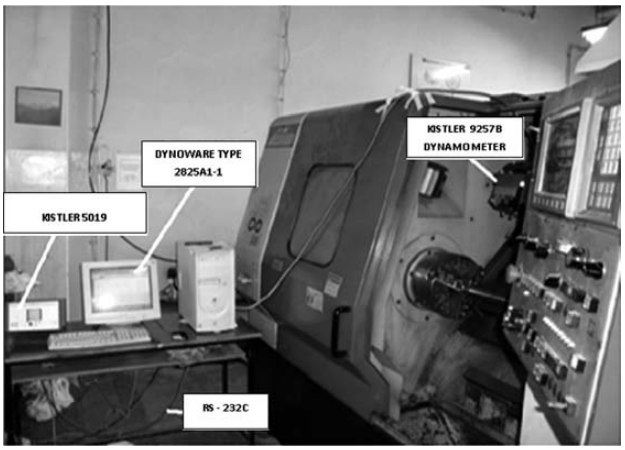

Figure 4: Experimental setup
Slika 4: Eksperimentalni sestav

related literature and the ISO 3685 standard. **Table 3** shows the types of cutting tool, tip radius, depth of cut, feed rate and cutting speed.

An industrial-type Johnford TC-35 CNC lathe was used as the machine tool. To measure the axial (*Fx*), radial (*Fy*) and main (*Fz*) cutting-force components, a KISTLER 9257B dynamometer was used. This dynamometer was connected with a KISTLER TYPE 5019 multichannel charge amplifier and the cutting-force signals were sent to a computer with an RS-232C cable connection. The graphs were obtained with the DynoWare Type 2825A1-2 software. F_x (F_a), F_y (F_r) and F_z (F_c) force values were determined during the machining processes. These values were calculated as the average scalar values in newtons (N) by the DynoWare software.

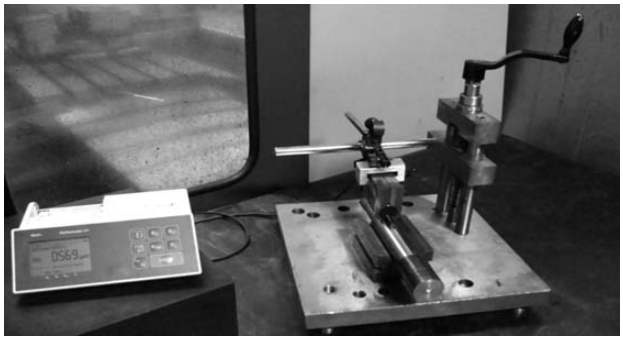

Figure 5: Surface-roughness measurement device
Slika 5: Naprava za merjenje hrapavosti površine

A schematic presentation of the experimental setup is shown in **Figure 3,** while the experimental setup is shown in **Figure 4**.

For the measurement of the surface-roughness values, a MAHR-Perthometer M1 model device was used (**Figure 5**). The cut-off length and the sampling length were chosen to be 0.8 mm and 5.6 mm, respectively. Three measurements were made parallel to the longitudinal axis of the workpiece at the intervals of 120°. The average surface roughness, R_a, was taken into account in all the measurements.

3 ARTIFICIAL NEURAL NETWORK MODEL

The concept of an artificial neural network has emerged with the idea that it simulates the operating principles of a human brain. The first studies were made with mathematical modeling of biological neurons that make up the brain cells. An artificial neural network consists of a large number of interconnected processing elements. Artificial neural network processing elements are called simple nerves.

An artificial neural network contains a large number of interconnected nodes. A nerve is the basic unit of an artificial neural network. An artificial nerve is, thus, simpler than a biological nerve. **Figure 6** shows an artificial neural network algorithm. All the artificial neural networks are derived from this basic structure. The differences in the structure of artificial neural networks result in different classification types.

The learning procedure can be affected by establishing correct correlations between the input and the output in artificial neural networks. This process falls below a certain value of the error between the foreseen output and the desired output. Artificial neural networks learn like a human. The more samples are used for learning, the more accurate is the obtained result. When a certain input is entered, the network can make changes to the data in order to give similarly accurate answers. The Levenberg-Marquardt (Levenberg, 1944; Marquardt, 1963) method uses a search direction that is a solution of the linear set of equations:

$$(J(x_k)^T J(x_k)+x_k I)d_k = -J(x_k)^T F(x_k) \quad (1)$$

or, optionally, of the equations:

$$(J(x_k)^T J(x_k)+l_k \operatorname{diag}(J(x_k)^T J(x_k)))d_k = \\ = -J(x_k)^T F(x_k) \quad (2)$$

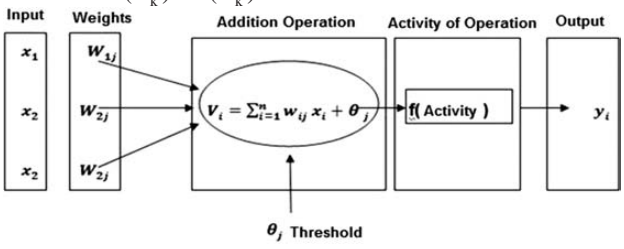

Figure 6: Artificial neural network
Slika 6: Umetna nevronska mreža

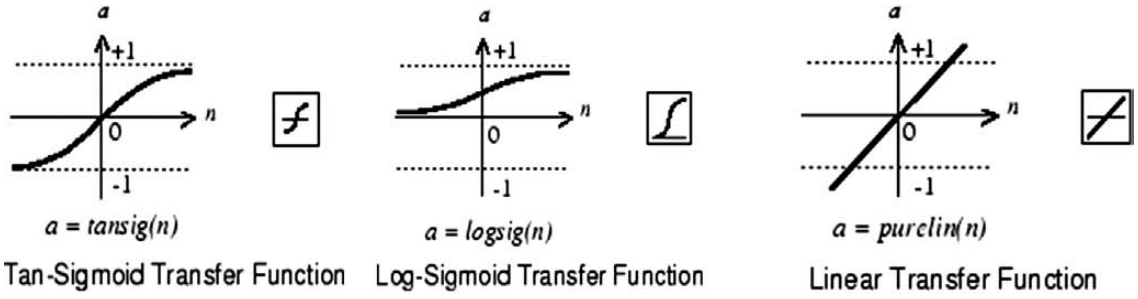

Figure 7: Used ANN functions
Slika 7: Uporabljene funkcije ANN

where scalar λ_k controls both the magnitude and direction of d_k. It is necessary to set the Scale Problem option to 'none' to choose Equation 1 and to 'Jacobian' to choose Equation 2.

Multilayer networks often use the log-sigmoid transfer function (logsig). The function generates the outputs between 0 and 1 as a neuron's net input goes from the negative to the positive infinity. Alternatively, multilayer networks can use the tan-sigmoid transfer function (tansig). Sigmoid output neurons are often used for pattern-recognition problems, while linear output neurons are used for function-fitting problems. The linear transfer function is shown below (**Figure 7**).

4 RESULTS AND DISCUSSIONS

4.1 Experimental study results

In this study, the influence of the machining parameters (cutting speed, feed rate and depth of cut) on the cutting forces (F_a, F_r and F_c) and surface-roughness values were investigated when machining the 50CrV4 (SAE 6150) steel. The surface-roughness values were analyzed on the basis of the process variables such as cutting speed, feed rate, depth of cut, and cutting-tool type. In addition, the influences of these variables on the cutting force were also examined. The relations between the cutting forces and the surface roughness were defined. A total of 270 experiments were performed to examine the effects of these variables. The minimum surface-roughness value was obtained with the coated cermet cutting tool, while the maximum surface-roughness value was obtained with the coated carbide cutting tool. The cutting-force components were measured (F_a, F_r, F_c). Maximum F_a, F_r and F_c were obtained with the coated carbide cutting tool. However, minimum F_a and F_r were obtained with the coated cermet cutting tool. Maximum R_a was obtained with the coated cermet cutting tool, while minimum Ra was obtained with the coated carbide cutting tool. A direct relation can be seen between the cutting forces and surface-roughness values. The lower are F_a and F_r, the lower are the surface-roughness values (**Table 4**).

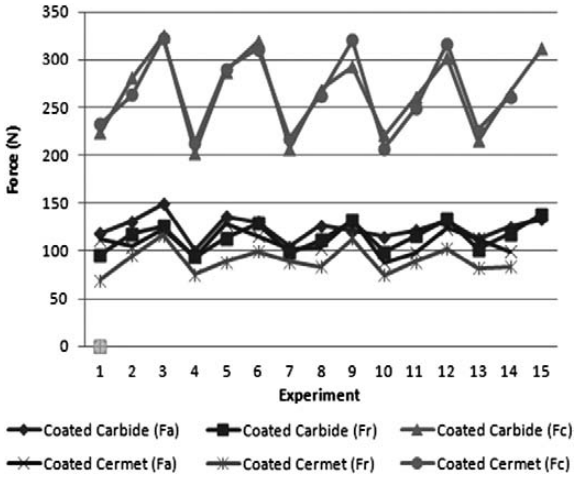

Figure 8: Comparison of the cutting forces: machining with coated carbide/cermet cutting tools
Slika 8: Primerjava sil pri rezanju: rezanje z orodjem s karbidno ali kermetno prevleko

Table 4: Maximum/minimum values of the cutting force and surface roughness
Tabela 4: Maksimalne/minimalne vrednosti sil pri rezanju in hrapavost površine

Cutting tool (coated carbide/cermet)	Cutting tool (z)	Depth of cut *d*/mm	Cutting speed *v*/(mm/min)	Feed rate *f*/(mm/r)	F_x (F_a)/N	F_y (F_r)/N	F_z (F_c)/N	Surface roughness R_a/μm	Min/max
Cermet	6	0.5	250	0.12	74.37	118.83	218.68	0.345	$F_{a\,min}$
Carbide	2	1.5	150	0.2	454.17	203.88	836.12	1.619	$F_{a\,max}$
Cermet	4	1.5	200	0.12	321.63	51.72	516.02	0.702	$F_{r\,min}$
Carbide	3	1.5	250	0.2	399.06	319.58	804.36	1.336	$F_{r\,max}$
Carbide	1	0.5	175	0.12	100.11	94.04	202.54	0.634	$F_{c\,min}$
Carbide	3	1.5	200	0.2	409.48	305.07	859.52	1.315	$F_{c\,max}$
Cermet	6	0.5	250	0.12	74.37	118.83	218.68	0.345	$R_{a\,min}$
Carbide	1	1.5	150	0.2	437.23	110.79	814.09	1.893	$R_{a\,max}$

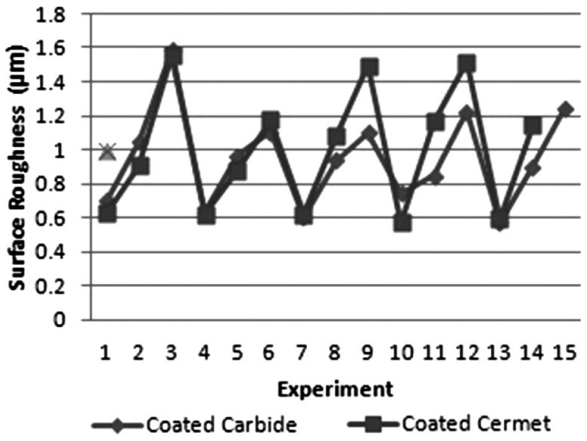

Figure 9: Comparison of the surface-roughness values: machining with coated carbide/cermet cutting tools
Slika 9: Primerjava vrednosti hrapavosti površine: rezanje z orodjem s karbidno ali kermetno prevleko

The cutting-force values were found to influence the resulting surface-roughness values. When F_a, F_r and F_c increase, the surface roughness also increases. There is a direct correlation between the F_a, F_r, F_c values and R_a. When the resulting surface-roughness values are examined, it is seen that the surface-roughness values obtained with the coated cermet cutting tools are lower than those obtained with coated carbide tools. The resultant force components of F_a, F_r and F_c have a direct correlation with R_a. Maximum F_a, F_r and F_c appeared with the coated carbide cutting tools (**Figure 8**). However, the minimum surface-roughness values were obtained with the coated cermet cutting tools (**Figure 9**). The lower surface-roughness values obtained with the coated cermet cutting tools can be explained with a lower built-up-edge (BUE) formation tendency of the cermet cutting tools. The presence of BUE on the cutting tool significantly increases the surface-roughness values.

4.2 Performance of the ANN model

An experimental design was accomplished. A 2^7 fully factorial experimental design was planned. Totally, 8 column × 270 line data was obtained from the experiments. This data was divided into groups. 70 % of the data was used for the training, 15 % of the data was used for the validation of the results and 15 % of the data was used to test the results. A multiple regression analysis was accomplished (R^2 = 0.81810949, adjusted

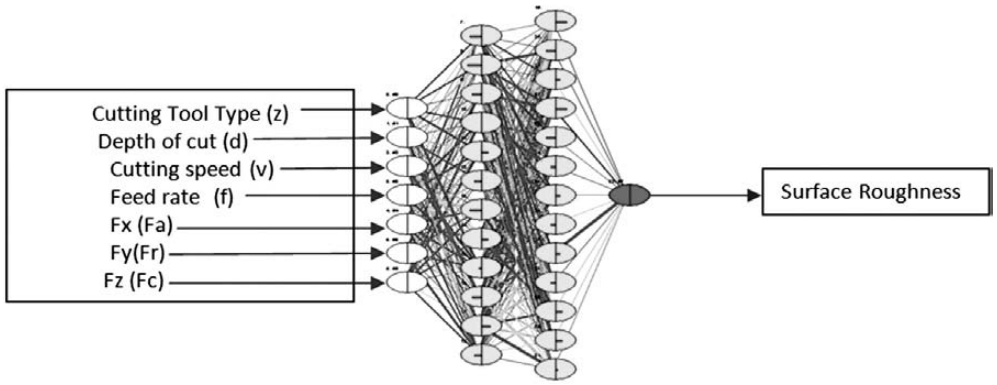

Figure 10: ANN model
Slika 10: ANN-model

Table 5: Iterations to find the best ANN model
Tabela 5: Približki pri iskanju najboljšega ANN-modela

Net name	Training performance	Test performance	Training error	Test error	Training algorithm
MLP 7-26-1	0.942287	0.910443	0.002352	0.003235	BFGS 52
MLP 7-14-1	0.957514	0.913514	0.001748	0.003132	BFGS 54
MLP 7-29-1	0.957661	0.911581	0.001738	0.003189	BFGS 90
MLP 7-26-1	0.940432	0.904966	0.002425	0.003485	BFGS 59
MLP 7-20-1	0.947744	0.907168	0.002135	0.003365	BFGS 73
MLP 7-54-1	0.960559	0.916491	0.001624	0.003013	BFGS 109
MLP 7-26-1	0.943531	0.910626	0.002302	0.003236	BFGS 50
MLP 7-37-1	0.987255	0.952368	0.000532	0.001757	BFGS 132
RBF 7-53-1	0.929539	0.905647	0.002851	0.003411	RBFT
MLP 7-50-1	0.955443	0.904887	0.001829	0.003456	BFGS 67
MLP 7-43-1	0.962073	0.909532	0.001561	0.003283	BFGS 52
MLP 7-74-1	0.944994	0.907058	0.002245	0.003363	BFGS 66
MLP 7-45-1	0.943063	0.908330	0.002321	0.003342	BFGS 52

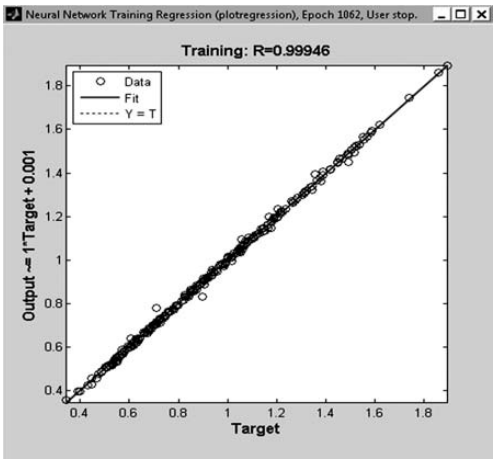

Figure 11: ANN training result
Slika 11: Rezultati ANN-usposabljanja

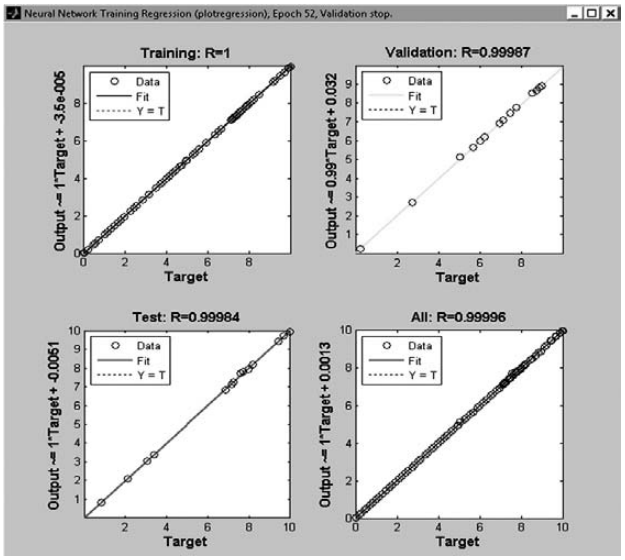

Figure 12: ANN results: training, validation and the test
Slika 12: Rezultati ANN: usposabljanje, ocena in preizkus

R^2 = 0.81324982). The results obtained with the multiple regression analyses were not enough to interpret the experiment results. For this reason, an Annova analysis was also performed. But Annova did not make any contribution towards interpreting the experimental results either. The Statistica software was used for the statistical analysis. The artificial neural network (ANN) model could not be improved. A code was developed for modeling the ANN using Matlab. Different ANN models were tried (**Table 5**) and the best ANN model with the highest learning level was chosen. The code used in the model resulted in very sound results (*RMS* = 0.0055829150, R^2 = 0.9997334826 and *MEP*/% = –0.0000134181). These are the average values of all the ANN-model results.

There are many commercial ANN software products. In this study, the Matlab neural network toolbox was used to obtain a neural network model. There are seven inputs (type of cutting tool, coated carbide/cermet cutting tools, depth of cut, cutting speed, feed rate, F_a, F_r, F_c forces and one output (surface roughness). A multi-layer feed-forward perceptron (MLP 12-13-1) was used in the ANN model. The tansig, logsig and purelin functions were used on the Matlab code and the Levenberg-Marquardt training method was used in the ANN model. **Figure 10** shows the ANN model.

Figure 11 shows the training performance of the model. According to the graphs, the training percentage is a maximum. This shows that the training value can be acceptable. The resulting value is very close to 1. **Figure 12** shows the ANN results: the training, validation and the test regression-analysis results. The performance of the ANN model relates to the deviation between the actual output values and predicted output values. **Table 6** shows a comparison of the experimental values and the Matlab neural-network predictions. The error amounts were used for the analysis of three statistical values.

Table 6: ANN test data
Tabela 6: Podatki ANN-preizkusa

Cutting tool (z)	Depth of cut *d*/mm	Cutting speed *v*/(mm/min)	Feed rate *f*/(mm/r)	F_x (F_a)/N	F_y(F_r)/N	F_z (F_c)/N	Experimental surface roughness (R_a/μm)	ANN model test (*MATLAB*)	*RMS*	R^2	*MEP*
1	0.5	150	0.12	118.5	95.61	224.01	0.708	0.703709	0.004291	0.999963	0.006097
1	0.5	150	0.16	130.96	118.18	280.97	1.046	1.041602	0.004398	0.999982	0.004223
2	1	175	0.12	235.44	163.89	403.76	0.603	0.604894	0.001894	0.99999	–0.00313
2	1	175	0.16	221.03	164.91	474.29	0.866	0.868187	0.002187	0.999994	–0.00252
2	1	175	0.2	237.59	177.01	567.95	1.106	1.103077	0.002923	0.999993	0.00265
3	0.5	200	0.16	83.21	155.97	249.81	0.711	0.713359	0.002359	0.999989	–0.00331
3	0.5	200	0.2	97.96	173.58	310.1	1.018	1.014781	0.003219	0.99999	0.003172
3	0.5	225	0.12	86.49	148.89	226.71	0.465	0.470102	0.005102	0.999882	–0.01085
4	0.5	225	0.2	123.95	102.78	316.82	1.515	1.502162	0.012838	0.999927	0.008546
4	0.5	250	0.12	113.08	82.18	226.48	0.596	0.582287	0.013713	0.999445	0.02355
4	0.5	250	0.2	121.36	121.4	301.84	1.568	1.565077	0.002923	0.999997	0.001868
5	0.5	250	0.2	92.58	126.44	292.2	1.387	1.385913	0.001087	0.999999	0.000784
5	1	150	0.12	204.73	134.97	394.89	0.637	0.636777	0.000223	0.999999	0.000351

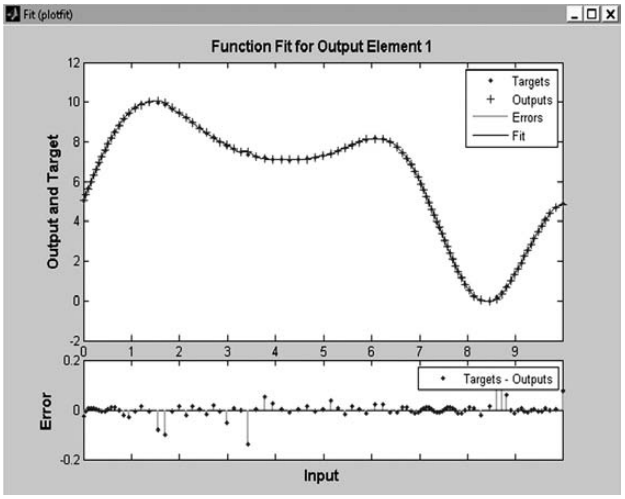

Figure 13: ANN function fit for the output
Slika 13: ANN-funkcja, primerna za izhod

Figure 13 shows ANN function fit for output. **Figure 14** shows ANN error histogram (30 Bins and 20 Bins). These are the statistical errors of the *RMSE* (the root mean square error), R^2 (the absolute fraction of variance)

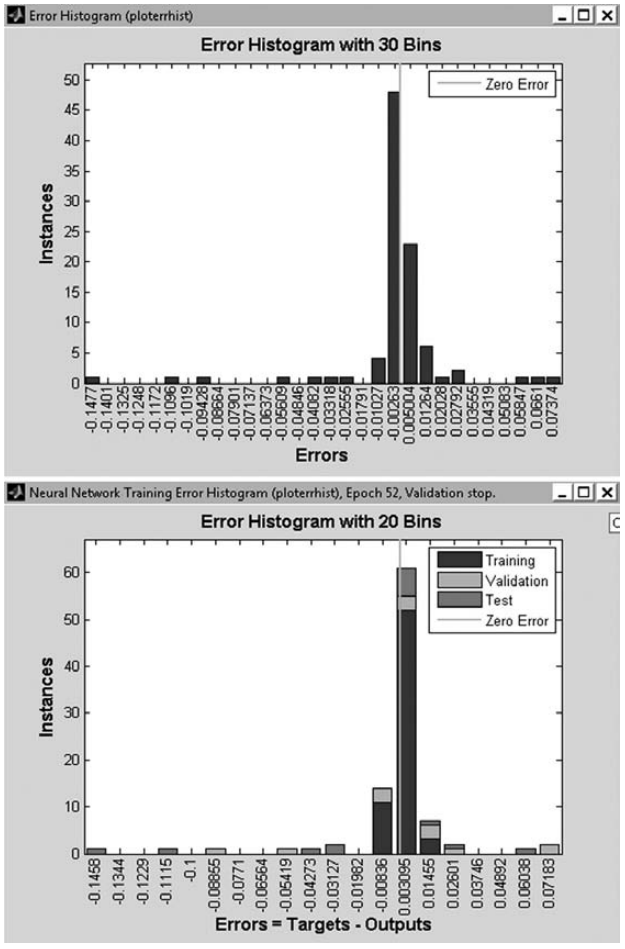

Figure 14: ANN error histograms, 30 Bins and 20 Bins
Slika 14: Histogram ANN-napak, 30 Bins in 20 Bins

and the *MEP* (the mean error percentage). If these error amounts are calculated according to the value of the output surface roughness, the *RMSE* is found to be smaller than 0.004291, R^2 is 0.999963 and the MEP is around 0.006097 for the training and test data.

The *RMSE*, R^2 and *MEP* values are obtainable with the following equations:

$$RMSE = \sqrt{\frac{1}{p}\sum j\left(t_j - o_j\right)^2} \tag{3}$$

$$RMSE = \sqrt{\left|0.708 - 0.703709\right|^2} = 0.004291$$

The statistical error amount:

$$R^2 = 1 - \frac{\sum j(t_j - o_j)^2}{\sum j(o_j)^2} \tag{4}$$

$$R^2 = 1 - \frac{(0.708 - 0.703709)^2}{(0.703709)^2} = 0.999963$$

and the average percent error:

$$MEP/\% = \frac{\sum j\left(\frac{t_j - o_j}{t_j}\cdot 100\right)}{p} \tag{5}$$

$$MEP/\% = \frac{0.708 - 0.703709}{0.703709}\cdot 100 = 0.006097$$

values are obtained, where t is the target value, o is the output and p is the number of the samples.

5 CONCLUSIONS

An ANN was developed for predicting the surface-roughness values in turning the 50CrV4 (SAE 6150) steel using the cutting forces (F_a, F_r and F_c) and machining parameters. The influences of the machining parameters (cutting speed, feed rate, depth of cut and cutting-tool material) on the cutting forces and surface roughness were investigated. The optimum configuration of the ANN consisted of three layers with the LM neural network approach. The statistical-analysis results are: *RMSE* = 0.004291, R^2 = 0.999963, *MEP*/% =0.006097. The predicted surface-roughness values using the ANN model are in good agreement with the experimentally obtained surface-roughness values. The ANN based on the calculation can be used to predict the surface roughness depending on the machining parameters. These results can be used to predict the cutting forces and surface roughness in machining the 50CrV4 (SAE 6150) steel using the coated carbide and cermet cutting tools. In conclusion, a surface-roughness prediction not requiring an experimental study with ANN models can provide both simplicity and fast calculation. It is shown that an ANN model can be used as an effective and alternative method of experimental studies improving both the time and economical optimization of the machining.

6 REFERENCES

[1] N. Boubekri, J. Rodriguez, S. Asfour, Development of an aggregate indicator to assess the machinability of steels, Journal of Materials Processing Technology, 134 (**2003**), 159–165

[2] A. S. Kumar, A. R. Durai, T. Sornakumar, Machinability of hardened steel using alumina based ceramic cutting tools, International Journal of Refractory Metals & Hard Materials, 21 (**2003**), 109–117

[3] Z. Tekiner, S. Yeşilyurt, Investigation of the cutting parameters depending on process sound during turning of AISI 304 austenitic stainless steel, Materials and Design, 25 (**2004**), 507–513

[4] J. G. Lima, R. F. Ávila, A. M. Abrão, M. Faustino, J. Paulo Davim, Hard turning: AISI 4340 high strength low alloy steel and AISI D2 cold work tool steel, Journal of Materials Processing Technology, 169 (**2005**), 388–395

[5] J. A. Arsecularatne, L. C. Zhang, C. Montross, Wear and tool life of tungsten carbide, PCBN and PCD cutting tools, International Journal of Machine Tools & Manufacture, 46 (**2006**), 482–491

[6] L. L. Qian, M. R. Hossan, Effect on cutting force in turning hardened tool steels with cubic boron nitride inserts, Journal of Materials Processing Technology, 191 (**2007**), 274–278

[7] A. Ebrahimi, M. M. Moshksar, Study of machinability in boring operation of microalloyed and heat-treated alloy steels, Materials Science and Engineering A, 460–461 (**2007**), 314–323

[8] S. K. Khrais, Y. J. Lin, Wear mechanisms and tool performance of TiAlN PVD coated inserts during machining of AISI 4140 steel, Wear, 262 (**2007**), 64–69

[9] R. Tanaka, Y. Yamane, K. Sekiya, N. Narutaki, T. Shiraga, Machinability of BN free-machining steel in turning, International Journal of Machine Tools & Manufacture, 47 (**2007**), 1971–1977

[10] Y. Işık, Investigating the machinability of tool steels in turning operations, Materials and Design, 28 (**2007**), 1417–1424

[11] P. J. Arrazola, I. Arriola, M. A. Davies, A. L. Cooke, B. S. Dutterer, The effect of machinability on thermal fields in orthogonal cutting of AISI 4140 steel, CIRP Annals – Manufacturing Technology, 57 (**2008**), 65–68

[12] R. Yiğit, E. Celik, K. F. Findik, S. Köksal, Effect of cutting speed on the performance of coated and uncoated cutting tools in turning nodular cast iron, Journal of Materials Processing Technology, 204 (**2008**), 80–88

[13] M. C. Cakir, Y. Isik, Investigating the machinability of austempered ductile irons having different austempering temperatures and times, Materials and Design, 29 (**2008**), 937–942

[14] D. I. Lalwani, N. K. Mehta, P. K. Jain, Experimental investigations of cutting parameters influence on cutting forces and surface roughness in finish hard turning of MDN250 steel, Journal of Materials Processing Technology, 206 (**2008**), 167–179

[15] T. V. SreeramaReddy, T. Sornakumar, M. VenkataramaReddy, R. Venkatram, Machinability of C45 steel with deep cryogenic treated tungsten carbide cutting tool inserts, Int. Journal of Refractory Metals & Hard Materials, 27 (**2009**), 181–185

[16] M. A. Xavior, M. Adithan, Determining the influence of cutting fluids on tool wear and surface roughness during turning of AISI 304 austenitic stainless steel, Journal of Materials Processing Technology, 209 (**2009**), 900–909

[17] A. Ebrahimi, M. M. Moshksar, Evaluation of machinability in turning of microalloyed and quenched-tempered steels: Tool wear, statistical analysis, chip morphology, Journal of Materials Processing Technology, 209 (**2009**), 910–921

[18] M. Nalbant, H. Gokkaya, I. Toktas, G. Sur, The experimental investigation of the effects of uncoated, PVD- and CVD-coated cemented carbide inserts and cutting parameters on surface roughness in CNC turning and its prediction using artificial neural networks, Robotics and Computer-Integrated Manufacturing, 25 (**2009**), 211–223

[19] V. N. Gaitonde, S. R. Karnik, L. Figueria, J. P. Davim, Machinability investigations in hard turning of AISI D2 cold work tool steel with conventional and wiper ceramic inserts, Int. Journal of Refractory Metals & Hard Materials, 27 (**2009**), 754–763

[20] D. G. Thakur, B. Ramamorthy, L. Vijarayaghavan, Study on the machinability characteristics of superalloy Inconel 718 during high speed turning, Materials and Design, 30 (**2009**), 1718–1725

[21] P. J. Arrazola, I. Arriola, M. A. Davies, Analysis of the influence of tool type, coatings, and machinability on the thermal fields in orthogonal machining of AISI 4140 steels, CIRP Annals – Manufacturing Technology, 58 (**2009**), 85–88

[22] K. Boucha, M. Y. Athmane, T. Mabrouki, F. J. Rigal, Statistical analysis of surface roughness and cutting forces using response surface methodology in hard turning of AISI 52100 bearing steel with CBN tool, Int. Journal of Refractory Metals & Hard Materials, 28 (**2010**), 349–361